

Towards Agility: A Momentum Aware Trajectory Optimisation Framework using Full-Centroidal Dynamics & Implicit Inverse Kinematics

Aristotelis Papatheodorou, Wolfgang Merkt, Alexander L. Mitchell, Ioannis Havoutis

Abstract—Online planning and execution of acrobatic maneuvers pose significant challenges in legged locomotion. Their underlying combinatorial nature, along with the current hardware’s limitations constitute the main obstacles in unlocking the true potential of legged-robots. This letter tries to expose the intricacies of these optimal control problems in a tangible way, directly applicable to the creation of more efficient online trajectory optimisation frameworks. By analysing the fundamental principles that shape the behaviour of the system, the dynamics themselves can be exploited to surpass its hardware limitations. More specifically, a trajectory optimisation formulation is proposed that exploits the system’s high-order nonlinearities, such as the nonholonomy of the angular momentum, and phase-space symmetries in order to produce feasible high-acceleration maneuvers. By leveraging the full-centroidal dynamics of the quadruped ANYmal C and directly optimising its footholds and contact forces, the framework is capable of producing efficient motion plans with low computational overhead. The feasibility of the produced trajectories is ensured by taking into account the configuration-dependent inertial properties of the robot during the planning process, while its robustness is increased by supplying the full analytic derivatives & Hessians to the solver. Finally, a significant portion of the discussion is centred around the deployment of the proposed framework on the ANYmal C platform, while its true capabilities are demonstrated through real-world experiments, with the successful execution of high-acceleration motion scenarios like the squat-jump.

Index Terms—trajectory optimisation, agile maneuvers, full-centroidal dynamics

I. INTRODUCTION

Agility in legged locomotion remains an intricate puzzle, primarily due to the complex nature of multi-contact Trajectory Optimisation (TO). The problem inherently has a combinatorial character, especially when considering articulated systems. Unlike their non-articulated counterparts, these systems have discrete contact points. The solver has to determine the sequence of these points, which in turn may not directly lead to a unique combination of limbs in contact for each timestep. On top of that, redundancy allows different configurations for a given task. However, the constraints determining the optimal one are often non-convex, leading to solutions susceptible to local minima.

In high-acceleration and underactuated scenarios, such as flight phases during jumps illustrated in Fig. 1, kinetic momentum and particularly its angular component, imposes a nonholonomic constraint intrinsic to rigid-body systems

All authors are with the Dynamic Robot Systems (DRS) group, Oxford Robotics Institute, University of Oxford. Email: {aristotelis,wolfgang,mitch,ioannis}@robots.ox.ac.uk.

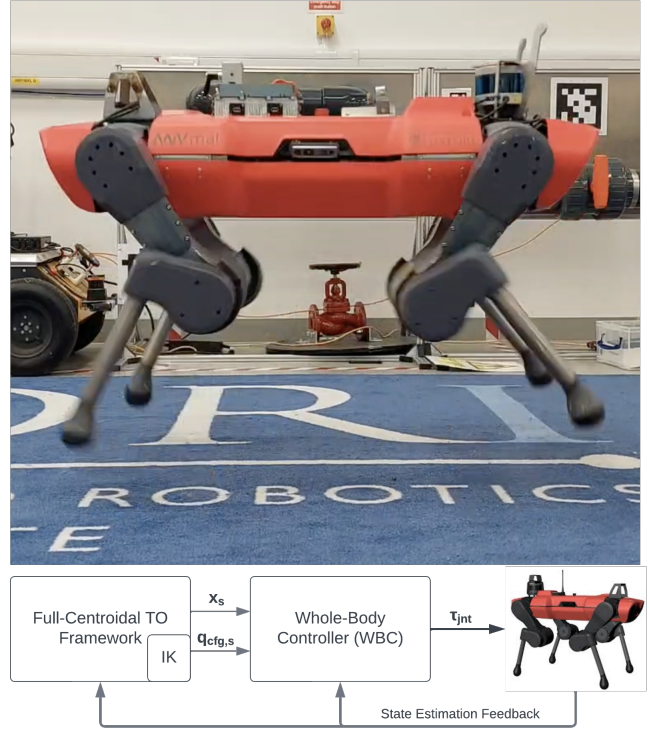


Fig. 1. ANYmal C performing a squat-jump: The proposed TO framework manages to overcome the limitations imposed by the high-mass of the robot and its low torque limits and successfully perform a jump. It’s worth to be noted that even though ANYmal’s WBC runs at 400Hz, it is neither designed nor tuned for that kind of tasks, hence its constraining trajectory tracking limitations had to be taken into account in deployment. The controller takes the desired state trajectory from the proposed TO framework and produces the required torques for the jump, while no re-planning is used to further highlight the ability of the proposed formulation to produce feasible, long-horizon trajectories.

[1]. Analysing the Newton-Euler equations in Eq. (1) for an arbitrary articulated system without external forces, reveals that the conservation of angular momentum allows precise orientation control. More specifically, the angular velocity ω_k of each body (out of N_b number of bodies), along with its mass (m_k), position (\mathbf{p}_k), velocity ($\dot{\mathbf{p}}_k$), and inertia (\mathbf{I}_k), as well as the system’s CoM position (\mathbf{p}_{CoM}) are inextricable quantities to the overall system’s rotation. Note that \mathbf{R}_k is the rotation matrix of the body.

It becomes apparent that by moving the limbs assymmetrically (gesticulation [2]), the system’s rotation can be controlled, since its total inertia is dependent on the configura-

tion of the limbs. Yet, accurately tracking and controlling inertia, while considering the articulated bodies' contributions, introduces an additional layer of computational complexity.

$$\begin{aligned} \sum_{k=0}^{N_b} (m_k) \dot{\mathbf{p}}_{CoM} &= \text{Constant} \\ \sum_{k=0}^{N_b} [(\mathbf{p}_k - \mathbf{p}_{CoM}) \times m_k \dot{\mathbf{p}}_k + \mathbf{R}_k \mathbf{I}_k \boldsymbol{\omega}_k] &= \text{Constant} \end{aligned} \quad (1)$$

In general, motions in legged robots are realised by them applying forces to their environment. These forces in addition to being nonlinearly coupled with the robot's actuated joints, they are subject to various constraints. For instance, their feasibility is governed by the unilateral force relationship with the ground and the motors' torque limits. Apparently, these limits impose restrictions on the robot's ability to execute high-acceleration maneuvers. However, nonholonomy again plays a role by allowing the system to build-up momentum and surpass its actuators' capabilities [3]. That is why accurate inertia tracking is of paramount importance.

Of course, Model Predictive Controllers (MPCs) are equipped to stabilize such systems [4], but all these physical phenomena result in huge computational overheads and non-convexities [5]. To highlight the complexity, even the most elaborate learning-based approaches [6], however their astonishing results, with all the robustness and generalisation that Deep Reinforcement Learning (DRL) agents come with, suffer from the plethora of different scenarios and tasks that may encounter. Hence, multiple ones are trained on different tasks, while their orchestration requires tedious tuning.

A. Related Work

Often researchers resort to simplifications, such as linearised centroidal dynamics models, to enforce convexity [5]. However, these fail to encapsulate the system's true nonlinearities, critical for dynamic stability during rapid maneuvers. Full Rigid-Body Dynamics (FRBD) approaches offer promise but suffer from slow convergence due to their inherent complexity and nonlinearity. Some innovative solutions have used an alternating optimisation paradigm, attempting dynamic consensus between a reduced-order model and FRBD [7] [8]. However, these approaches do not come without their set of complications. The alternating optimisation cycles, along with the inertia-dependent dynamic consensus constraints impose a performance overhead, challenging the feasibility of real-time application. Moreover, as the time-horizon increases, the growing dimensions of the Karush-Kuhn-Tucker (KKT) matrix challenge general-purpose solvers, leading to slower convergence rates.

Differential Dynamic Programming (DDP) has emerged as a solution, excelling in performance by breaking down the problem into simpler sequences [9]. In particular, this family of indirect TO methods exploits the inherent markovian structure [10] of the dynamics, avoiding the inversion of the full-KKT matrix, effectively reducing the computational complexity and large-matrix factorisations. The downside of such methods is that in their classic formulation they

cannot handle constraints. Modern approaches have modified the algorithm to handle some types of constraints [11] [12] and further improve convergence, since the cost function is not filled with penalty terms. Up until now, Box-FDDP [11], a state-of-the-art DDP solver with first-order Gauss-Newton approximation handles efficiently control-input box constraints. Hence, the state-dependent dynamic consensus constraints that the alternating optimisation methods rely on to achieve accurate momentum tracking are handled as penalty terms even by the most advanced DDP solvers, adding another layer of intricacy.

B. Contributions

This letter unveils a trajectory optimisation framework designed for the quadruped robot ANYmal C [13], emphasizing its real-time capabilities for agile-maneuvers. It comes as a proof of concept with various novelties that enable the creation of a fully-fledged MPC framework in the future. Herein the alternating optimisation paradigm is avoided by using the full Centroidal Dynamics of the robot. The solver directly optimises the footholds and contact forces, the fundamental quantities that generate the motion in articulated systems. This in turn minimises the effect that the nonlinear coupling between the actuated joints and the contact forces has in the problem's resolution, making motion-planning more intuitive and efficient. At the same time, to have accurate momentum tracking the analytic Inverse Kinematics (IK) and their derivatives are calculated implicitly, thus not affecting the dimensionality of the problem. To solve it, the Box-FDDP solver is chosen, since it comes with a better globalisation strategy than classical DDP solvers and can handle box constraints in the control-inputs. Any other state-dependent constraints are added as penalty terms. To alleviate the implications of that, all the derivatives of the dynamics and cost function, along with the required Hessians are provided to the solver analytically. To the best of our knowledge, this is the first time that the Hessian of the $\mathbb{SE}(3)$ [14] group's Difference operator (\ominus) is provided analytically, which provably yields faster convergence (see Section III) as the task complexity increases. Since the whole framework is designed with performance in mind, all quantities are calculated from scratch without using any FRBD algorithms such as Recursive Newton Euler Algorithm (RNEA) [15]. Hence, a novel way to efficiently calculate the inertia tensor derivatives has been created that can be parallelised to further increase its performance. Last, the framework has been realised in *Python 3* using *Pinocchio* [16] and *Crocodyl* [17] for prototyping, and deployed in *C++* to highlight its performance capabilities. To sum-up this work introduces:

- A Full Centroidal Dynamics TO framework with analytic IK that accurately tracks momentum and executes planning of agile-maneuvers in an online fashion
- A Comprehensive derivation of all analytic derivatives and Hessians for cost and dynamics, devoid of simplifications and approximations
- A versatile TO framework adaptable to various robot architectures with minimal changes

C. Paper Outline

The current letter is organised as follows: (i) Section II highlights the methods and the technical details of the framework, (ii) Section III discusses the benchmarks employed to showcase the framework’s capabilities along with some details about the systematic tuning of such tasks, and (iii) Section IV addresses concluding remarks and future work.

II. METHOD

The overall architecture of the proposed locomotion pipeline in Fig. 1 relies on two modules: (a) the Full-Centroidal TO framework for efficiently planning trajectories, and (b) the Whole-Body-Controller (WBC) of the ANYmal C [18] that executes these motion plans. While creating a time-varying feedback policy based on the derived DDP gains offers certain benefits [3], its inclusion is beyond the scope of this letter. The complexities of synchronisation and real-time tuning of such a framework warrant a dedicated exploration, while they would have rendered the novelties of the proposed TO formulation insufficiently addressed.

A. Problem Formulation

Given a predefined sequence of contact points and durations, the Optimal Control Problem (OCP) is illustrated in Eq. (2). The time-horizon of the OCP is discretised in N timesteps, the contributions of which are summed, to come with the total cost. The state and control-input terms are standard LQR costs. The goal is to find the optimal sequence of control-inputs \mathbf{u}_s^* that minimises the cost and respects the given constraints.

$$\min_{\mathbf{u}_s \in \mathcal{U}} \sum_{k=0}^{N-1} \left[\left\| \mathbf{x}_k^{ref} \ominus \mathbf{x}_k \right\|_{\mathbf{Q}_k}^2 + \left\| \mathbf{u}_k^{ref} - \mathbf{u}_k \right\|_{\mathbf{R}_k}^2 + l_{kin,k} + l_{fr,k} \right]$$

s.t.:

$$\mathbf{x}_{k+1} = \mathbf{x}_k \oplus \int_{t_k}^{t_k+dt} \mathbf{f}(\mathbf{x}_k, \mathbf{u}_k) dt \quad (\text{Dynamics})$$

$$\underline{\mathbf{u}} \leq \mathbf{u} \leq \bar{\mathbf{u}} \quad (\text{Control-Input Bounds}) \quad (2)$$

where:

$$\begin{aligned} \mathbf{x} &= (\mathbf{p}_b, \mathbf{q}_o, \mathbf{v}_b, \boldsymbol{\omega}, \mathbf{r}_{LF}, \mathbf{r}_{LH}, \mathbf{r}_{RF}, \mathbf{r}_{RH}) \in \mathcal{X} \\ \mathbf{u} &= (\mathbf{F}_{LF}, \dot{\mathbf{r}}_{LF}, \mathbf{F}_{LH}, \dot{\mathbf{r}}_{LH}, \mathbf{F}_{RF}, \dot{\mathbf{r}}_{RF}, \mathbf{F}_{RH}, \dot{\mathbf{r}}_{RH}) \in \mathcal{U} \end{aligned} \quad (3)$$

The state vector \mathbf{x} in Eq. (3) lies on the differentiable manifold of the admissible states ($\mathcal{X} \subseteq \mathbb{SE}(3) \times \mathbb{R}^{18}$) and comprises the Cartesian position and orientation of the base-origin ($\mathbf{p}_b, \mathbf{q}_o$) $\in \mathbb{SE}(3)$, the corresponding base velocities ($\mathbf{v}_b, \boldsymbol{\omega}$) $\in \mathbb{R}^6$ and each foothold’s 3D-position for the Left-Fore (\mathbf{r}_{LF}), Left-Hind (\mathbf{r}_{LH}), Right-Fore (\mathbf{r}_{RF}) and Right-Hind (\mathbf{r}_{RH}) legs. Moreover, the control-input vector \mathbf{u} in Eq (3) lies on the Euclidean manifold of admissible controls ($\mathcal{U} \subseteq \mathbb{R}^{24}$), and consists of each foothold’s contact force (\mathbf{F}) and Cartesian velocity ($\dot{\mathbf{r}}$). Note that the state is a Lie-Group [14] and as such, it satisfies different axioms and operations from the Euclidean ones, such as the Integration (\oplus) and Difference (\ominus) operations [19]. Lastly, it does

not include footholds’ velocities, effectively reducing the problem’s dimensions.

The kinematic reachability term ($l_{kin,k}$) penalises the footholds that violate the robot’s workspace ($l_{eff,max}$). Essentially, a weighted quadratic-barrier function discourages infeasible leg-configurations as shown in Eq. (4), where $\mathbf{r}_{HAA \rightarrow Foot}$ represents each leg’s effective length.

$$l_{kin,k} = \frac{1}{2} \mathbf{dr}_k^T \mathbf{H}_k \mathbf{dr}_k, \text{ with: } k \in [0, N)$$

where:

$$\mathbf{dr}_k = \max \left[\begin{pmatrix} \left(\left\| \mathbf{r}_{LF, HAA \rightarrow Foot} \right\| - l_{eff,max} \right) \\ \vdots \\ \left(\left\| \mathbf{r}_{RH, HAA \rightarrow Foot} \right\| - l_{eff,max} \right) \end{pmatrix}, \mathbf{0} \right]_k \in \mathbb{R}^4 \quad (4)$$

Finally the friction-cone penalty ($l_{fr,k}$) ensures that the solution does not violate the Coulomb-friction constraint for the n_c feet in contact. The term illustrated in Eq. (5) is an overapproximation of the friction-cone that provably has better convergence and less computational cost [5].

$$\begin{aligned} l_{fr,k} &= \frac{1}{2} \sum_{i=0}^{n_c-1} \left[\left(\left| F_{i,x} \right| - \mu F_{i,z} \right)^+ \right]^2 \\ &\quad + \left(\left| F_{i,y} \right| - \mu F_{i,z} \right)^+ \right]^2 \Big|_k, \\ \text{with: } (\dots)^+ &= \max((\dots), 0) \ \& \ k \in [0, N) \end{aligned} \quad (5)$$

B. Dynamics Model

As previously mentioned, the Full-Centroidal Dynamics model used in this letter (see Eq. (6)) encapsulates all of the system’s nonlinearities and the nonholonomic constraint of angular momentum. The used inertia has no simplifications, while no FRBD algorithm is used for the calculation of its terms. The model has a translational part shown in Eq. (6a) and a rotational one in Eq. (6b).

$${}^W \dot{\mathbf{v}}_{CoM} = \frac{1}{m} \sum_{i=0}^{n_c-1} ({}^W \mathbf{F}_i) + {}^W \mathbf{g} \quad (6a)$$

$$\begin{aligned} {}^W \dot{\boldsymbol{\omega}} &= {}^W \mathbf{I}(\mathbf{q}_{cfg})^{-1} [-{}^W \boldsymbol{\omega} \times ({}^W \mathbf{I}(\mathbf{q}_{cfg}) {}^W \boldsymbol{\omega}) \\ &\quad + \sum_{i=0}^{n_c-1} [({}^W \mathbf{r}_i - {}^W \mathbf{p}_{CoM}(\mathbf{q}_{cfg})) \times {}^W \mathbf{F}_i]] \end{aligned} \quad (6b)$$

The translational part is simply Newton’s Second-Law, calculating the translational acceleration of the robot’s CoM (${}^W \dot{\mathbf{v}}_{CoM}$) in which ${}^W \mathbf{g}$ represents the gravitational acceleration expressed in the World frame (W). On the other hand, the rotational part in Eq. (6b) is not that simple. The calculation of the angular acceleration (${}^W \dot{\boldsymbol{\omega}}$) not only imposes the nonholonomy to the dynamics, but also major nonlinearities manifest, such as the coupling of the contact forces with the CoM and footholds’ positions and the highly nonlinear configuration-dependent inertia matrix. It becomes obvious that in order to calculate the inertia, the configuration of the robot’s legs (\mathbf{q}_{cfg}) is necessary. However, including it in the state of the system would have not only been redundant, but also it would have increased the dimensionality of the OCP

significantly. Instead, the closed-form IK could be used. That does not restrict the framework, since most quadrupeds have 3-joint legs susceptible to analytic IK solutions. In the current letter the implementation of the *Xpp* library [20] is used for the quadruped ANYmal C. According to Eq. (7), given the current state of the system, the algorithm can produce the joint angles of the robot's legs.

$$\mathbf{q}_{cfg,k} = \mathbf{IK}(\mathbf{x}_k), \text{ with: } k \in [0, N] \quad (7)$$

Ultimately, the Dynamics constraint of the OCP (Eq. (2)) is composed as in Eq. (8) and lives in the Euclidean tangent-space (\mathcal{T}_x) of the admissible states. More specifically, the control-input directly affects the footholds, which in turn, along with the contact forces, affect the CoM's dynamics (see Eq. (6)).

$$\dot{\mathbf{x}} = \mathbf{f}(\mathbf{x}, \mathbf{u}) = \begin{pmatrix} {}^B \mathbf{v}_b \\ {}^B \boldsymbol{\omega} \\ {}^B \dot{\mathbf{v}}_b \\ {}^B \dot{\boldsymbol{\omega}} \\ {}^W \dot{\mathbf{r}}_{LF} \\ {}^W \dot{\mathbf{r}}_{LH} \\ {}^W \dot{\mathbf{r}}_{RF} \\ {}^W \dot{\mathbf{r}}_{RH} \end{pmatrix} \in \mathcal{T}_x \subseteq \mathbb{R}^{24} \quad (8)$$

However, the translational acceleration of the CoM has to be projected to the base-origin of the robot (${}^B \dot{\mathbf{v}}_b$) expressed in its body-fixed frame (B). The formula in Eq. (9) approximates this projection by neglecting some minor gyroscopic terms that do not affect the result, given that the relative acceleration and velocity of the CoM to the robot's base-origin remains low, which in most scenarios is the case. The alternative would be to utilise a FRBD algorithm of *Pinocchio* to calculate the missing terms, but that comes with significant computational overhead and thus rejected.

$${}^B \dot{\mathbf{v}}_b = {}^B \mathbf{R}_W {}^W \dot{\mathbf{v}}_{CoM} + ({}^B \mathbf{R}_W {}^W \dot{\boldsymbol{\omega}}) \times {}^B \mathbf{p}_{CoM \rightarrow b} \quad (9) \\ + {}^B \boldsymbol{\omega} \times ({}^B \boldsymbol{\omega} \times {}^B \mathbf{p}_{CoM \rightarrow b}) - {}^B \boldsymbol{\omega} \times {}^B \mathbf{v}_b$$

C. Calculation of Derivatives

DDP is a gradient-based method. Hence, the state and control-input derivatives of the dynamics and cost, along with the cost's Hessians are required. In a nutshell, the solver approximates the cost with a linear quadratic function and, ultimately, finds the descend direction in each iteration. The inherent limitation of the Box-FDDP solver means it cannot handle state-dependent constraints explicitly, so kinematic reachability and friction-cone constraints must be encoded as penalties, adding complexity and sensitivity to the cost function. In order to have robust convergence and increase the overall performance of the algorithm, the analytic derivatives and Hessians are calculated and provided to the solver. Deriving these derivatives and encoding them efficiently to minimise their computational burden has been proved to be challenging. First of all, the state-vector does not include the velocities of the footholds, hence a new custom *Crocodyl* action model had to be implemented. Moreover, the library's symplectic Euler integration has been employed, a

simple variational integrator [21] that conserves the system's geometric properties and phase-space symmetries, ensuring enhanced energy conservation during integration.

Second, the state derivatives reside in the tangent space \mathcal{T}_x . Most tangent-space first-order derivatives (e.g. for the Integration and Difference operators) are well documented in the literature [19], while *Pinocchio* provides efficient implementations. However, the state cost-term requires the hessian of the Difference operator in order to come with the analytic hessian of the overall cost function. None of the available frameworks and publications [16] [19] provide an implementation, while its effect on convergence has not been documented before. To start with, the first-order derivative of the state cost-term is calculated as shown in Eq. (10), where \otimes designates the Hamilton product [22].

$$l_x = (\mathbf{x}^{\text{ref}} \ominus \mathbf{x})^T \mathbf{Q} \frac{D\ominus}{D\mathbf{x}},$$

$$\text{where: } \frac{D\ominus}{D\mathbf{x}_{\mathbb{SE}3}} = -\mathbf{J}_{1,\mathbb{SE}3}^{-1}(\boldsymbol{\tau}),$$

$$\text{with: } \boldsymbol{\tau} = (\mathbf{p}, \boldsymbol{\theta}) = \mathbf{x}_{\mathbb{SE}3}^{\text{ref}} \ominus \mathbf{x}_{\mathbb{SE}3} = \mathbf{Log}(\mathbf{x}_{\mathbb{SE}3}^{-1} \otimes \mathbf{x}_{\mathbb{SE}3}^{\text{ref}}) \quad (10)$$

Note that the derivative of the Difference operator is non-trivial only for the $\mathbb{SE}(3)$ elements of the state (i.e. $\mathbf{x}_{\mathbb{SE}3}$), hence Eq. (11) shows the derivation only for these elements. Note that $(\mathbf{p}, \boldsymbol{\theta})$ represent the tangent-space lie-algebra vectors of the manifold [19]. These vectors are related to the base's position and orientation with the Exponential and Logarithmic mappings. Furthermore, the left-Jacobian ($\mathbf{J}_{1,\mathbf{q}_o}$) of the quaternion (\mathbf{q}_o), along with matrix \mathbf{Q} are derived in [19].

$$\mathbf{J}_{1,\mathbb{SE}3}^{-1}(\boldsymbol{\tau}) = \begin{pmatrix} \mathbf{J}_{1,\mathbf{q}_o}^{-1}(\boldsymbol{\theta}) & \mathbf{J}_{1,\mathbf{q}_o}^{-1}(\boldsymbol{\theta}) \mathbf{Q}(\boldsymbol{\tau}) \mathbf{J}_{1,\mathbf{q}_o}^{-1}(\boldsymbol{\theta}) \\ \mathbf{0} & \mathbf{J}_{1,\mathbf{q}_o}^{-1}(\boldsymbol{\theta}) \end{pmatrix} \quad (11)$$

By differentiating Eq. (10) again, the hessian of the state-cost term is derived in Eq. (12). Even though the Difference operator's hessian is a tensor, its sparsity could be leveraged to come with an efficient implementation. The effect of the Hessian to convergence is illustrated in Fig. 2 for a variety of tasks created to benchmark the framework. Further details on the tasks can be found in Section III.

$$l_{xx} = \frac{D\ominus}{D\mathbf{x}}^T \mathbf{Q} \frac{D\ominus}{D\mathbf{x}} + (\mathbf{x}^{\text{ref}} \ominus \mathbf{x})^T \mathbf{Q} \frac{D^2\ominus}{D\mathbf{x}^2} \quad (12) \\ \frac{D^2\ominus}{D\mathbf{x}_{\mathbb{SE}3}^2} = \frac{\partial}{\partial \boldsymbol{\tau}} \left(-\mathbf{J}_{1,\mathbb{SE}3}^{-1}(\boldsymbol{\tau}) \right) \frac{D\ominus}{D\mathbf{x}_{\mathbb{SE}3}}$$

Finally, the inertia matrix's derivatives posed a significant challenge. In any rigid-body system, the total inertia can be calculated by sequentially projecting each body's inertia to a specified frame (e.g. body-fixed frame) and accumulating their contributions with a weighted sum. Hence, the derivative of the system's inertia is retrieved by differentiating these projections w.r.t. the legs' configuration (\mathbf{q}_{cfg}) and summing them. However, by exploiting the articulated nature of the system, these computations can be parallelised to calculate each leg's inertia simultaneously. Ultimately, to come up with

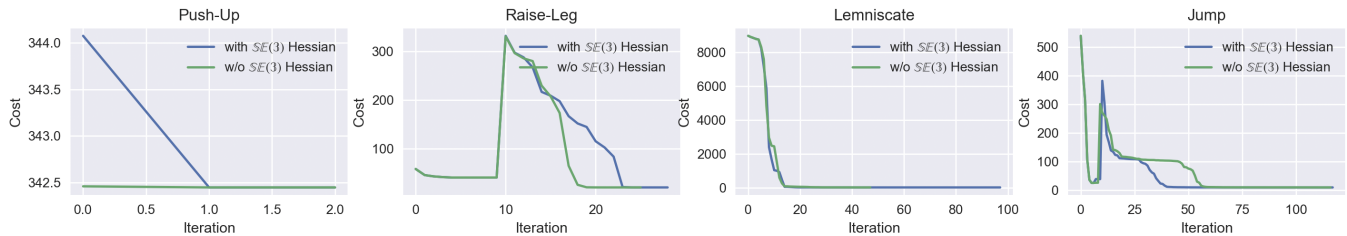


Fig. 2. $SE(3)$ Hessian Impact on Convergence: As the task complexity increases, the impact of the tangent-space hessian on the convergence becomes more significant. Even in the simpler tasks, the hessian leads to better optimal-cost value and stricter constraint satisfaction. Hence, the kinematic-reachability and friction-cone constraints are satisfied better, while the overall convergence is more robust to initial conditions. It becomes apparent that early stopping can be used to decrease the iterations of the algorithm.

the derivatives w.r.t. the system’s state \mathbf{x} , the closed form IK are auto-differentiated using CasADi [23]. The resulting tangent-space derivatives are computed using the chain-rule as shown in Eq. (13). Once again, their sparsity could be leveraged to optimise their runtime.

$$\frac{D^B \mathbf{I}}{D\mathbf{x}} = \frac{d^B \mathbf{I}}{d\mathbf{q}_{cfg}} \frac{D\mathbf{q}_{cfg}}{D\mathbf{x}} \quad (13)$$

To avoid kinematic singularities and prevent irregular configurations and derivatives, a workspace violation avoidance mechanism is employed. Essentially, the foothold that violates the robot’s kinematic constraint is normalised to be inside the effective workspace of the leg, as shown in Eq. (14). Then the modified state is fed into the IK algorithm.

$$\begin{aligned} {}^W \mathbf{r}_{HAA \rightarrow FOOT, mod} &= \frac{{}^W \mathbf{r}_{HAA \rightarrow Foot}}{\|{}^W \mathbf{r}_{HAA \rightarrow Foot}\|} l_{eff, max} \Rightarrow \\ {}^W \mathbf{r}_{Foot, mod} &= {}^W \mathbf{r}_{HAA} + {}^W \mathbf{r}_{HAA \rightarrow Foot, mod} \end{aligned} \quad (14)$$

III. RESULTS & DISCUSSION

The framework is evaluated through some carefully designed benchmarks that highlight its capabilities and place it in direct comparison with the current state-of-the-art [2] [3] [7]. Towards this, real-world experiments of three tasks with incremental complexity were executed. The proposed TO framework was able to plan feasible, long-horizon trajectories that include high-accelerations and abrupt changes in motion direction. Even though that larger horizons are generally welcome in MPC frameworks, they downgrade performance and make the solution more sensitive to initial conditions. Arguably, the proposed formulation has been more than capable to address these intricacies by effectively planning highly dynamic motions. Of course the use of ANYmal’s WBC is a limiting factor, since it considers a simplified model and rewrites the dynamics of the desired state-space trajectory. However, its inherent reactivity due to its high control-loop frequency partially alleviates its shortcomings.

To tune the tasks, the Weights & Biases (wandb) [24] hyperparameter optimisation package has been used. Its Bayesian optimisation [25] module was utilised to find a close-to-optimal solution for the weights, while the kinematic reachability and Coulomb friction constraints were fine-tuned manually afterwards for best performance. Arguably

by defining a more elaborate minimization function, the manual fine-tuning step could be eliminated entirely. Each task offers a unique perspective into the framework’s capabilities and highlights the contributions referenced in Section I-B.

A. Push Up

The push-up showcases the configuration dependent CoM of the robot and was initially used to verify the correctness of the approach. The planned trajectory resulted in a smooth, even motion of the robot’s base, while the steady-state contact forces were not entirely symmetrical as expected. This is due to the non-uniform weight distribution of the quadruped’s base, verifying the momentum tracking capabilities of the proposed TO framework.

B. Lemniscate Tracking

In this task the robot does not break contact with the ground. Even though it seems trivial, the ”8-like” motion of the base highlights the ability of the planned trajectory to respect the imposed penalty-constraints, since the CoM is positioned near the margins of the legs’ stability polygon without violating kinematic or friction-cone constraints. Non momentum-aware controllers could not realise such trajectory, since they assume fixed position of the robot’s CoM w.r.t. its base-origin, hence they do not have accurate control authority over its actual position.

C. Squat Jump

The squat-jump is designed to stress ANYmal’s WBC to the limit of its torque and speed capabilities. This proved to be very demanding, since the robot has significantly higher mass and more restrictive joint-torque limits, compared to the ones that have demonstrated similar behaviours in the past [7]. The whole task consists of an abrupt jumping motion that requires the solver to plan a squat trajectory in order to gain the required momentum, since the power of its actuators alone does not suffice. To maintain stability, the legs have to be moved accordingly in order to sustain correct orientation and base-height recovery during the landing phase. The weights of the different task phases are tuned using bayesian optimisation and then manually fine-tuned to better comply with the kinematic reachability and Coulomb friction constraints. The time-horizon of the task is 6.02s and its real-world experimental results are illustrated in Fig.3 .

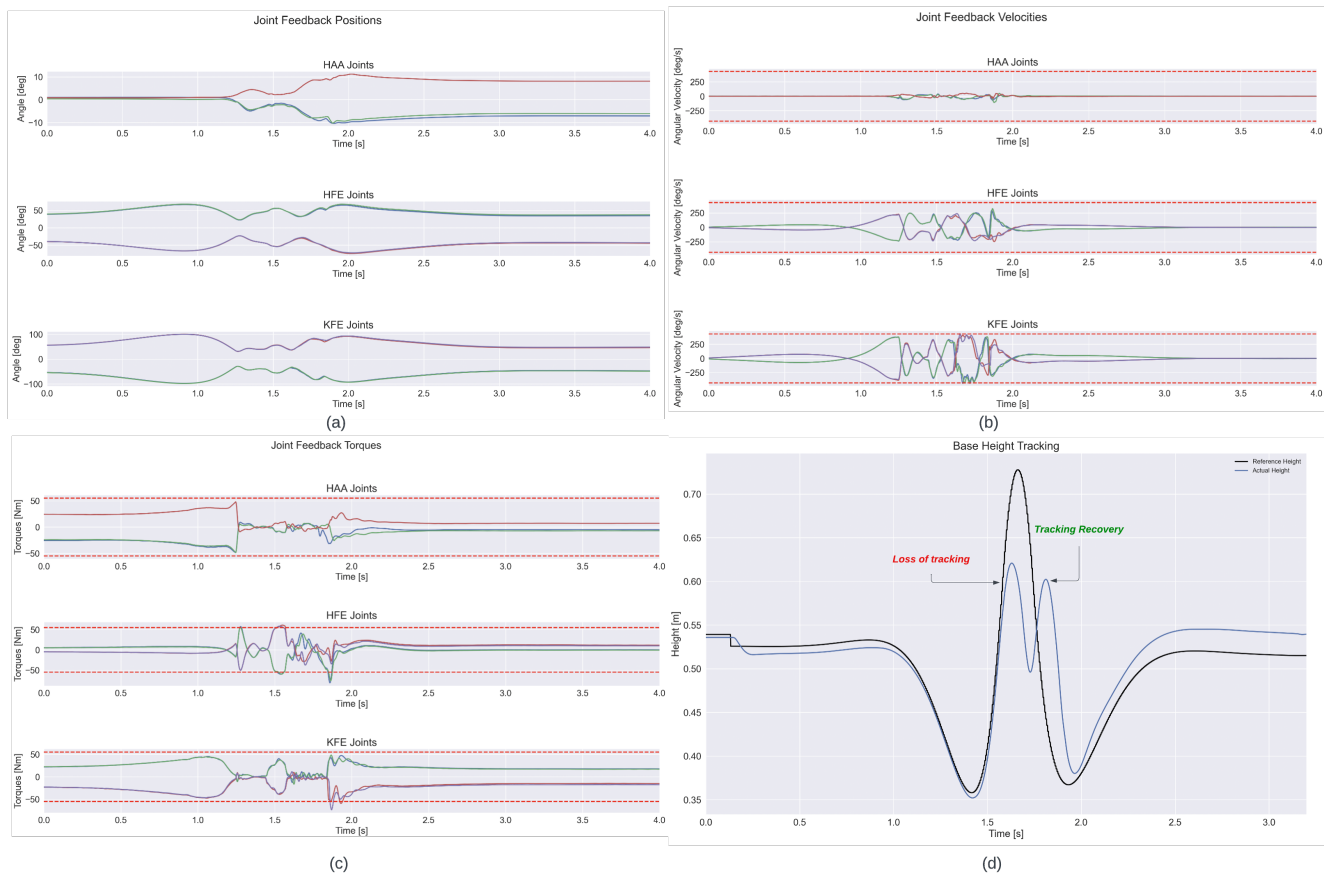


Fig. 3. Real-World Squat-Jump Indicative Results: The planned trajectory resulted in smooth feedback joint-angles (a) and no violations in the feedback joint-velocities (limit: 430 deg/s) as illustrated in (b). Moreover, the joint-torques are overall smooth, except of the touchdown that certain peaks violate the 55 Nm torque limit of the robot due to severe impact with the ground. Note that the torques are actually saturated at 80 Nm but for safety reasons the WBC has stricter constraints. Finally, in (c) the base height tracking is illustrated. Note that the WBC is not designed to track such motions and fails to follow the planned trajectory even though the accelerations are not high. The overall results come as proof that a fully-fledged MPC with the proposed TO formulation will be able to leverage the true capabilities of the ANYmal C platform, overcoming its high mass and low torque limits.

IV. CONCLUSION & FUTURE WORK

The quest for enhanced agility in legged robots, particularly within the realm of trajectory optimisation, remains a challenging endeavour. This paper presented a comprehensive trajectory optimisation framework tailored for the quadruped, ANYmal C. By leveraging the full Centroidal Dynamics and incorporating the analytic IK implicitly, the proposed methodology overcomes many of the shortcomings inherent in existing approaches. The adoption of the Box-FDDP solver, combined with the direct optimisation of footholds and contact forces, offers a promising direction for achieving agile maneuvers. The presented innovations not only enhance convergence but also provide a more intuitive planning process.

Several areas merit further investigation in the context of this work. Evaluating the framework’s real-time capabilities and creating an optimised MPC that bypasses ANYmal’s simplified WBC will be a key area of focus, since rewriting the trajectory with a simplified WBC violates the non-holonomic constraint in the dynamics and proved incapable of tracking the system’s momentum accurately. Hence, the

advantages of the current approach are partially diminished. Towards this, there are adaptations that can be made to the Box-FDDP solver to incorporate more hard-constraints and enhance its overall performance.

Finally, it will also be essential to understand the impact of environmental variables, such as diverse terrains and dynamic obstacles, on the presented method. Integration with perceptive or other sensory inputs for real-time trajectory adaptation, and a deeper exploration into the trade-offs between computational efficiency and planning accuracy, will certainly be of interest, since the overall formulation can be easily converted to an adaptive complexity MPC framework as proposed in [26]. It is certain that there are multiple routes to follow with vast interconnections, however continued research in these directions will undoubtedly expand the horizons of legged locomotion and combined with learning-based methods may prove to be the key to animal-level agility.

REFERENCES

- [1] P.-B. Wieber, *Holonomy and Nonholonomy in the Dynamics of Articulated Motion*, 07 2007, vol. 340, pp. 411–425.

- [2] R. Budhiraja, J. Carpentier, and N. Mansard, "Dynamics consensus between centroidal and whole-body models for locomotion of legged robots," in *2019 International Conference on Robotics and Automation (ICRA)*, 2019, pp. 6727–6733.
- [3] C. Mastalli, W. Merkt, G. Xin, J. Shim, M. Mistry, I. Havoutis, and S. Vijayakumar, "Agile maneuvers in legged robots: a predictive control approach," 2022.
- [4] R. W. Brockett, "Asymptotic stability and feedback stabilization," 1982. [Online]. Available: <https://api.semanticscholar.org/CorpusID:119958643>
- [5] T. Corbères, T. Flayols, P.-A. Léziart, R. Budhiraja, P. Souères, G. Saurel, and N. Mansard, "Comparison of predictive controllers for locomotion and balance recovery of quadruped robots," in *2021 IEEE International Conference on Robotics and Automation (ICRA)*, 2021, pp. 5021–5027.
- [6] D. Hoeller, N. Rudin, D. Sako, and M. Hutter, "Anymal parkour: Learning agile navigation for quadrupedal robots," 2023.
- [7] Z. Zhou, B. Wingo, N. Boyd, S. Hutchinson, and Y. Zhao, "Momentum-aware trajectory optimization and control for agile quadrupedal locomotion," *IEEE Robotics and Automation Letters*, vol. 7, no. 3, pp. 7755–7762, 2022.
- [8] Z. Zhou and Y. Zhao, "Accelerated admm based trajectory optimization for legged locomotion with coupled rigid body dynamics," in *2020 American Control Conference (ACC)*, 2020, pp. 5082–5089.
- [9] D. Jacobson and D. Mayne, *Differential Dynamic Programming*, ser. Modern analytic and computational methods in science and mathematics. American Elsevier Publishing Company, 1970. [Online]. Available: <https://books.google.co.uk/books?id=tA-oAAAAIAAJ>
- [10] P. A. Gagnic, "Markov chains: From theory to implementation and experimentation," 2017. [Online]. Available: <https://api.semanticscholar.org/CorpusID:86648212>
- [11] C. Mastalli, W. Merkt, J. Marti-Saumell, J. Solà, N. Mansard, and S. Vijayakumar, "A direct-indirect hybridization approach to control-limited DDP," *CoRR*, vol. abs/2010.00411, 2020. [Online]. Available: <https://arxiv.org/abs/2010.00411>
- [12] W. Jallet, N. Mansard, and J. Carpentier, "Implicit differential dynamic programming," in *2022 International Conference on Robotics and Automation (ICRA)*, 2022, pp. 1455–1461.
- [13] M. Hutter, C. Gehring, D. Jud, A. Lauber, C. D. Bellicoso, V. Tsounis, J. Hwangbo, K. Bodie, P. Fankhauser, M. Bloesch, R. Diethelm, S. Bachmann, A. Melzer, and M. Hoepflinger, "Anymal - a highly mobile and dynamic quadrupedal robot," in *2016 IEEE/RSJ International Conference on Intelligent Robots and Systems (IROS)*, 2016, pp. 38–44.
- [14] J. Stillwell, *Naive Lie Theory*, ser. Undergraduate Texts in Mathematics. Springer New York, 2008. [Online]. Available: <https://books.google.co.uk/books?id=SuR5OAgxyDIC>
- [15] R. Featherstone, *Rigid Body Dynamics Algorithms*. Springer US, 2014. [Online]. Available: <https://books.google.co.uk/books?id=GJRGBQAAQBAJ>
- [16] J. Carpentier, G. Saurel, G. Buondonno, J. Mirabel, F. Lamiroux, O. Stasse, and N. Mansard, "The pinocchio c++ library : A fast and flexible implementation of rigid body dynamics algorithms and their analytical derivatives," in *2019 IEEE/SICE International Symposium on System Integration (SII)*, 2019, pp. 614–619.
- [17] C. Mastalli, R. Budhiraja, W. Merkt, G. Saurel, B. Hammoud, M. Naveau, J. Carpentier, S. Vijayakumar, and N. Mansard, "Crocodyl: An efficient and versatile framework for multi-contact optimal control," *CoRR*, vol. abs/1909.04947, 2019.
- [18] C. D. Bellicoso, F. Jenelten, C. Gehring, and M. Hutter, "Dynamic locomotion through online nonlinear motion optimization for quadrupedal robots," *IEEE Robotics and Automation Letters*, vol. 3, no. 3, pp. 2261–2268, 2018.
- [19] J. Solà, J. Deray, and D. Atchuthan, "A micro lie theory for state estimation in robotics," *CoRR*, vol. abs/1812.01537, 2018.
- [20] "Xpp dynamic motions library," <https://github.com/leggedrobotics/xpp>, accessed: 2010-09-30.
- [21] M. West, "Variational Integrators," Ph.D. dissertation, California Institute of Technology, Jun. 2004. [Online]. Available: <https://resolver.caltech.edu/CaltechETD:etd-06072004-161416>
- [22] Y.-B. Jia, "Quaternions and rotations *," 2015. [Online]. Available: <https://api.semanticscholar.org/CorpusID:7075201>
- [23] J. A. E. Andersson, J. Gillis, G. Horn, J. B. Rawlings, and M. Diehl, "CasADi – A software framework for nonlinear optimization and optimal control," *Mathematical Programming Computation*, vol. 11, no. 1, pp. 1–36, 2019.
- [24] "Weights & biases hyperparameter tuning software," <https://wandb.ai>, accessed: 2010-09-30.
- [25] D. Barber, *Bayesian reasoning and machine learning*. Cambridge ; New York: Cambridge University Press, 2012.
- [26] J. Norby, A. Tajbakhsh, Y. Yang, and A. M. Johnson, "Adaptive complexity model predictive control," 2022.